ELSEVIER

Journal of Power Sources 58 (1996) 231–234

JOURNAL OF POWER SOURCES

Short Communication

# Characteristics of pyrolyzed phenol–formaldehyde resin as an anode for lithium-ion batteries

Biying Huang [a], Yuzhen Huang [a], Zhaoxiang Wang [a], Liquan Chen [a,1], Rongjian Xue [a], Fosong Wang [b]

[a] *Institute of Physics, Academia Sinica, PO Box 603, Beijing, 100 080 People's Republic of China*
[b] *Chinese Academy of Sciences, Beijing, 100 864 People's Republic of China*

Received 19 October 1995; accepted 15 January 1996

**Abstract**

Polyacenic semiconductor (PAS) is obtained by pyrolyzing phenol–formaldehyde resin (PFR). The properties of PFR heat-treated at different temperatures are investigated. The lithium intercalation capacity of PAS as a function of heat-treatment temperature (HTT) exhibits a maximum at around 700 °C. A knee appears at 700 °C, not only in the plot of atomic ratio [H]/[C] versus HTT, but also in the plot of conductivity versus HTT. For PAS with a HTT of 700 °C, the maximum in the ratio of the relative intensity of Raman spectra at 1360 $cm^{-1}$ corresponds to nanometer graphite, and that at 1580 $cm^{-1}$ to graphite. A reasonable explanation of these phenomena is the transformation of nanometer graphite to graphite.

*Keywords:* Resins; Phenol–formaldehyde; Lithium-ion batteries; Anodes

## 1. Introduction

In spite of the high energy density of rechargeable lithium batteries, commercialization is impeded by the dendritic growth of metallic lithium during the cycling process. The latter results in cycle-life and serious safety problems. Materials that enable lithium-ion intercalation at low potentials overcome this problem and can be used with benefit as anodes in 'lithium-ion' batteries [1]. Some carbonaceous materials have been reported [2–4] to be extremely suitable for this purpose. In recent years, carbon-based materials have been extensively studied [5,6] as the anodes for lithium-ion batteries.

It has been demonstrated that polyacenic material can be electrochemically doped with lithium to form n-type semiconductor in a reversible manner, and that it can store and deliver electrical energy [7–9]. This paper reports a study of polyacenic semiconductor (PAS), a pyrolyzed phenol–formaldehyde resin (PFR).

## 2. Experimental

PAS was prepared by pyrolyzing phenol–formaldehyde resin at various temperatures, with a rate of temperature rise of 10 °C $h^{-1}$, under a nitrogen atmosphere [10]. The products were black porous material. The lithium intercalation capacity of PAS was determined by measuring the discharge capacity of an Li/PAS cell with a discharge current density of 0.4 mA $cm^{-2}$. The PAS electrodes were made by mixing the PAS powder with 5 wt.% Teflon powder and then pressing under a pressure of 10 MPa into a disk of diameter 10 mm and thickness 0.13 mm. The conductivity of PAS was measured with a 4192A LF impedance analyser. The contents of elemental hydrogen and carbon in the PAS sample were determined by atomic absorption spectroscopy.

The reported IR spectra were recorded with Alpha Centaurt FT-IR-type IR spectrometer.

Back-scattering Raman spectra were recorded with a Spex-1403 spectrometer. The radiation line was 488.0 nm. The power from the argon laser was 400 mW with a radiation spot of 0.2 mm diameter on the sample. The data were sampled and analysed with a Datamate system.

## 3. Results and discussion

The IR spectra of PFR and PFR heat-treated at different temperatures are shown in Fig. 1. For PFR heat-treated at 500 °C, the intensity of the stretching band of the –OH group of

[1] Senior author.


*PII* S0378-7753(96)02373-1

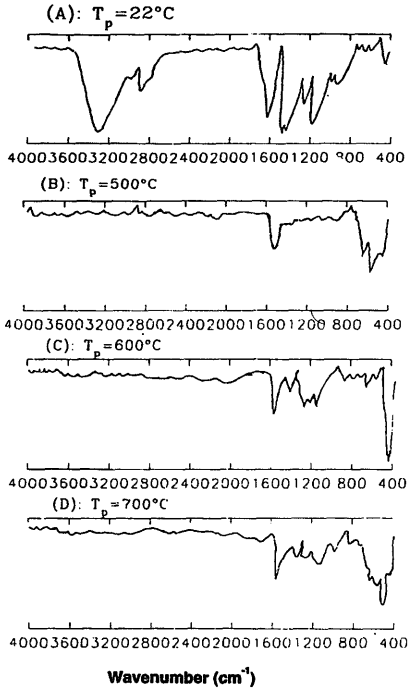


Fig. 1. IR spectra of PFR pyrolyzed at various temperatures.

PFR at 3380 and 1470 $cm^{-1}$ is greatly decreased, or even disappears. The 1224 $cm^{-1}$ band of the =C–O on the aromatic ring behaves similarly. Except for the band groups in the ranges 1053 to 1125 $cm^{-1}$ and 743 to 878 $cm^{-1}$, which are assigned to $\beta_{-CH}$ of the aromatic ring and the $\nu_{-CH}$ $n_{-CH}$ substituted benzene, respectively, and the $\nu_{-CH}$ vibration bands at 1628 $cm^{-1}$ and 737 to 864 $cm^{-1}$, all other bands disappear. For the sample treated at 700 °C, except for the $\nu_{-CH}$ band of the aromatic ring at 1628 $cm^{-1}$, all other bands disappear completely. All these results indicate clearly that during the pyrolysis process, PFR first undergoes intermolecular dehydration and, with increase in temperature, intramolecular dehydrogenation occurs. The latters leads to further carbonizing. Finally, only the polymerized aromatic rings are preserved.

The lithium intercalation capacity of PAS as a function of heat-treatment temperature (HTT) is shown in Fig. 2. The capacity increases with pyrolysis temperature and reaches a maximum value of 438 mAh $g^{-1}$ at about 700 °C. Thereafter, the capacity decreases.

The elemental ratio of [H]/[C] versus HTT is given in Fig. 3. At first, the ratio rapidly decreases. Above 700 °C, however, the ratio declines less dramatically.

The conductivity of PAS samples increases quickly with rise in the HTT up to 700 °C, then it changes smoothly, and then rapidly increases. Finally, the conductivity increases only slightly with temperature, see Fig. 4.

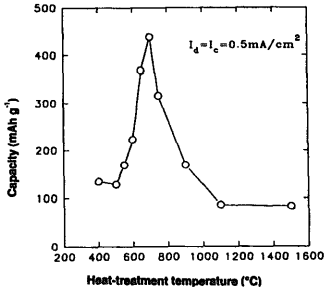


Fig. 2. Lithium intercalation capacity of PAS as a function of heat-treatment temperature.

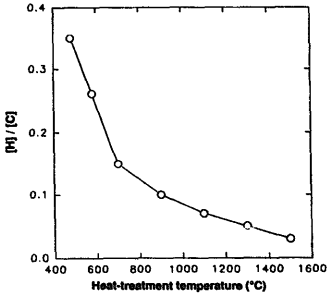


Fig. 3. Elemental ratio of [H]/[C] vs. heat-treatment temperature.

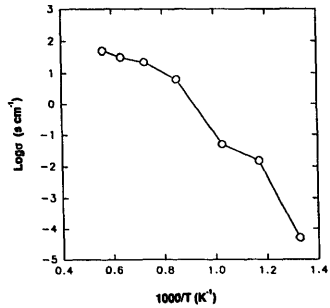


Fig. 4. Conductivity of PAS samples as a function of heat-treatment temperature.

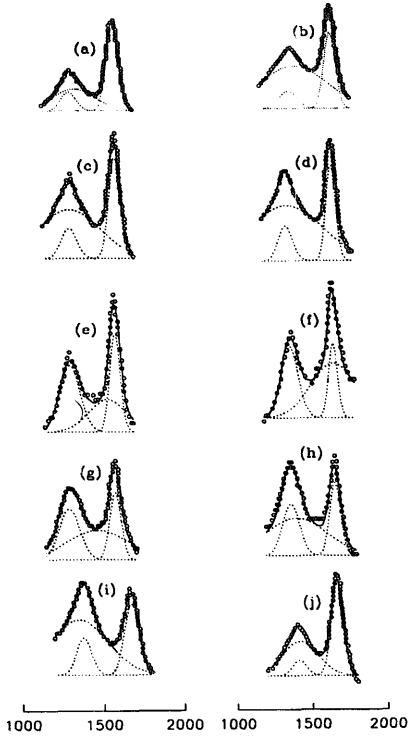


Fig. 5. Raman spectra of PAS heat treated at various temperatures. Open circles are experimental data, solid lines are fitting results, and dashed line is the three-fitting Raman line for each Raman spectra. (a) 400 °C; (b) 500 °C; (c) 550 °C; (d) 600 °C; (e) 650 °C; (f) 700 °C; (g) 750 °C; (h) 900 °C; (i) 1100 °C, and (j) 1500 °C.

All the PAS samples described in this work have three characteristic modes in the Raman spectra, see Fig. 5. One is around 1580 $cm^{-1}$ and corresponds to graphite; it is called the G-mode. The second is located around 1360 $cm^{-1}$ and is related to nanometer graphite; it is called the D-mode. The third covers a large range from 1300 to 1600 $cm^{-1}$ and may be attributed to the aromatic molecules; it is called the P-mode. According to Tuinstra and Koenic [11], the G-mode is associated with the 'in plane' atomic displacements in the central parts of large graphite crystallites, while the D-mode is caused by tiny crystallites or the boundaries of the larger crystallites. The P-mode may be related to the aromatic molecules that remain in the heat-treated samples. For discussion purposes, the portions in the samples that exhibit G-mode, D-mode and P-mode behaviour are called phase G, phase D and phase P, respectively.

Phase D can be considered as the clusters of two or three hexagonal carbon atom rings packed in parallel. The typical size of the clusters is several nanometers. Therefore, phase D is a nanometer graphite. By combining more hexagonal carbon layers, the nanometer graphite can become a larger graphite crystallite, phase G. Under thermal treatment, the aromatic molecules become hexagonal carbon atom rings, while phase P is the precursor of phase D. The plot of relative intensity $I_D/I_G$ as a function of HTT is shown in Fig. 6. It can be seen that a maximum appears when the sample is heat-treated at 700 °C.

The above results indicate that 700 °C is a critical HTT. What happens, therefore, at 700° C? The answer must lie in the structure and phase change in the PAS samples during the heat-treatment processes. From the Raman spectra of a PAS sample heat-treated at 400 °C (the lowest temperature used this study), it can be seen that both the graphite and the nanometer graphite are already present. Of course, the host phase (phenol–formaldehyde), and its evolutionary phases (aromatic molecules) also exist. Therefore, all the PAS samples heat-treated at various temperatures are mixed phases of graphite, nanometer graphite and aromatic molecules. The differences between the samples heat-treated at the various temperatures are determined by the relative content of these phases and their microstructure.

In the temperature range 400 to 700 °C, the pyrolysis reaction of phenol–formaldehyde progresses quickly with rise in temperature. Normally, during this process, the intermolecular dehydration and intramolecular dehydrogenation occur rapidly. Concomitantly, some aromatic molecules combine to form nanometer graphite. When the temperature reaches 700 °C, the amount of nanometer graphite becomes maximum and the speed of conversion from nanometer graphite to graphite increases. As a result, the ratio $I_D/I_G$ of the Raman spectra has a maximum when the temperature is 700 °C.

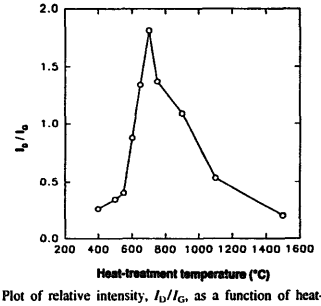


Fig. 6. Plot of relative intensity, $I_D/I_G$, as a function of heat-treatment temperature.

For the same reason, turning points appear in the curves of [H]/[C] and conductivity as a function of temperature, see Figs. 3 and 4.

Why does the PAS heat-treated at 700 °C have the highest lithium-intercalation capacity? The main phase is nanometer graphite accompanied by some graphite phase and a few aromatic molecules. Both nanometer graphite and graphite can accept lithium ions. Nanometer graphite consists of tiny graphite crystallites constructed with a few graphite rings. Besides the normal position for lithium ions in the first-stage intercalation graphite compound, there are large amounts of surface carbon atoms, that could become the position for lithium ions. Therefore, the lithium intercalation capacity for PAS heat-treated at 700°C can be as high as 438 mAh $g^{-1}$.

## Acknowledgements

The financial support from Ford and NSFC under contract No. 09 412 303 is gratefully acknowledged.

## References

[1] M. Mohri, N. Yanagisawa, Y. Tajima, H. Tanaka, T. Mitaie, S. Nakajima, Y. Yoshimoto, T. Suzuki and H. Wada, *J. Power Sources, 26* (1989) 545.
[2] J.O. Besenhard and H.P. Fritz, *Angew. Chem. Int. Ed. Engl., 22* (1983) 950.
[3] T. Nagaura and K. Tozawa, *Prog. Batteries Solar Cells, 9* (1990) 209.
[4] R. Fong, U. Von Sacken and J.R. Dahn, *J. Electrochem. Soc., 137* (1990) 2009.
[5] J. Yamaura, Y. Ozaki, A. Morita and A. Ohta, *J. Power Sources, 43* (1993) 233.
[6] K. Sekai, H. Azuma, A. Omaru, S. Fujita, H. Imoto, T. Endo, K. Yamaura, Y. Nishi, S. Mashiko and M. Yokogawa, *J. Power Sources, 43* (1993) 241.
[7] K. Tanaka, K. Ohzeki, T. Yamabe and S. Yata, *Synth. Met., 9* (1984) 41.
[8] S. Yata (Kanebo Ltd.), *EP Patent No. 0 067 444.*
[9] K. Tanaka, S. Yamanaka, T. Yamabe, K. Yoshino, G. Ishii and S. Yata, *Phys. Rev. B, 32* (1985) 6675.
[10] S. Yata, Y. Hato, K. Sakurai, H. Satake, K. Mukai, K. Tanaka and T. Yamabe, *Synth. Met., 18* (1990) 169.
[11] F. Tuinstra and J.L. Koenic, *J. Chem. Phys., 53* (1970) 126.